The Role of Spatial Frequency in Cuteness Discrimination of Infant Faces: An EEG Study

Mengni Zhou[1,2+] (zhoumengni@tyut.edu.cn), Runan Ding[3+] (2023510380@link.tyut.edu.cn)
Yanqing Dong[3] (dongyanqing0078@link.tyut.edu.cn), Xin Wen[1] (xwen@tyut.edu.cn)
Jie Xiang[3*] (xiangjie@tyut.edu.cn)
[1]College of Software, Taiyuan University of Technology
[2]Research Center for Medical Artificial Intelligence, Shenzhen Institute of Advanced Technology, Chinese Academy of Sciences
[3]College of Computer Science and Technology (College of Data Science), Taiyuan University of Technology
[+] equal contribution

Abstract

Infant facial cuteness serves as an evolutionary mechanism to enhance survival prospects by eliciting caregiving behaviors in adults. Spatial frequency (SF) processing is the basic mechanism for visual analysis. However, how different SFs contribute to the neural mechanisms underlying cuteness discrimination of infant faces remains poorly understood. To address this question, this study investigated how low SF (LSF) and high SF (HSF) differently modulate cuteness discrimination by behavioral accuracy measurement, event-related potential (ERP), time-frequency and functional connectivity analysis on recorded electroencephalogram (EEG) signals. Thirty participants performed a paired-comparison task in which they selected the cuter one face from two infant faces filtered with broad SF (BSF), LSF-only, or HSF-only. The behavioral results indicated that participants' cuteness discrimination ability in BSF condition was higher than that in LSF and HSF conditions. Time domain analysis revealed LSF faces elicited larger P1 amplitudes, while HSF faces evoked enhanced N170 and P300 components. Time-frequency and functional connectivity analyses further identified stronger theta-band oscillations and increased theta-band connectivity in posterior area when HSF faces were presented. These findings provide novel insights into the neural mechanisms underlying cuteness discrimination and highlight the importance of SFs integration in social face processing.

Keywords: cuteness; spatial frequency; ERP; time-frequency analysis; functional connectivity

Introduction

Cuteness is a pervasive phenomenon observed across both animate and inanimate entities (Borgi, Cogliati-Dezza, Brelsford, Meints, & Cirulli, 2014; Zhou et al., 2023). The prevailing view of cuteness can be traced back to baby schema (kindchenschema), proposed by Lorenz in 1943 (Lorenz, 1943). It refers to a set of infantile features (e.g., large eyes, a small nose and mouth, a large head, a high forehead, etc.) that are universally perceived as cute. These features are especially evident in human infants. Extensive behavioral and neuroimaging studies have demonstrated that cute infants can not only attract our attention (Kringelbach et al., 2008; Parsons et al., 2013; Senese et al., 2013; Thompson-Booth et al., 2014), but also evoke a range of emotional and caregiving behaviors. On one hand, cuteness can trigger positive emotional reactions (Almanza-Sepúlveda et al., 2018; Miesler, Leder, & Herrmann, 2011) and more nuanced feelings such as sympathy and tenderness (T. Wang, Mukhopadhyay, & Patrick, 2017). On the other hand, it can stimulate protective and nurturing behaviors in adults (Jia, Park, & Pol, 2015; Zhang & Zhou, 2020). Given that the survival of human infants heavily relies on the care and protection provided by others, understanding the cuteness processing mechanisms, particularly in the context of infant faces, is of significant interest. This study, therefore, focuses on exploring the neural processes involved in the cuteness processing of infant faces.

The face is a complex visual stimulus that requires the integration of both global and detailed information for comprehensive perception (Maurer, Le Grand, & Mondloch, 2002). These two types of facial information are encoded in different spatial frequency (SF) ranges. High SF (HSF) conveys fine details, while low SF (LSF) captures global information (Freeman & Loschky, 2011; Jennings, Yu, & Kingdom, 2017; Williams, Willenbockel, & Gauthier, 2009). A substantial body of evidence suggests that distinct SFs information is not always equally useful during the task execution. Instead, humans often selectively utilize the most paramount information depending on the goal of subtask at hand (T. Lin, Zhang, Fields, Sekuler, & Gutchess, 2022; Proverbio & Zani, 2021). Obviously, cuteness processing is involved in the encoding of facial information. However, the temporal course of how different SFs contribute to cuteness discrimination between two infant faces is still not fully comprehended.

Previous studies have shown that the time course of both face perception with different SFs information and social information comparison-related (e.g., trustworthiness) processes take effect within 200 milliseconds after individuals encounter stimulus (Han et al., 2022; H. Lin & Liang, 2024, 2025; Ohmann, Stahl, Mussweiler, & Kedia, 2016). During this early stage, a posterior P1 component emerges, followed by classical posterior N170 component. The P1 component, which emerges around 100 ms post-stimulus, is generally more sensitive to LSF information, as LSF facilitates rapid global processing and attention capture (Han et al., 2022; H. Lin & Liang, 2024; H. Wang, Lian, Wang, Chen, & Liu, 2023). The subsequent N170 component, peaking around 170 ms, is associated with the fine structural encoding of faces and is particularly sensitive to HSF information (Di Lorenzo et al., 2021; Han et al., 2022; H. Lin & Liang, 2024). Following this, the P300 component, which begins around 250 ms, reflects decision-making processes and is thought to be modulated by HSF, as it supports detailed evaluation and discrimination (Pfabigan et al., 2018; Proverbio, Cerri, & Gallotta, 2023; Shah et al., 2018; Wu, Zhang, Elieson, & Zhou, 2012).

In D. Barner, N.R. Bramley, A. Ruggeri and C.M. Walker (Eds.), *Proceedings of the 47th Annual Conference of the Cognitive Science Society*

Based on these established findings, we hypothesized that during cuteness discrimination task, LSF faces would elicit significantly enhanced P1 amplitude responses compared to HSF faces, reflecting their advantage in early global processing. Conversely, HSF faces were expected to evoke greater N170 and P300 amplitude responses relative to LSF faces, highlighting their role in fine structural encoding and subsequent evaluative decision-making processes.

In addition to event-related potential (ERP), electroencephalogram (EEG) signals also encompass oscillatory activity within specific frequency bands. Notably, theta-band oscillations (4-8 Hz) have been associated with face perception and emotion processing across multiple studies (Bossi et al., 2020; Dravida, Ono, Noah, Zhang, & Hirsch, 2019; Torrence, Troup, Rojas, & Carlson, 2021). Particularly, posterior theta-band oscillations have been identified as a neural marker for rapid, early-stage perceptual processing of highly salient stimuli (Dravida et al., 2019; Yang, Qiu, & Schouten, 2015). More importantly, evidence suggests that theta-band oscillations are sensitive to facial stimuli with distinct SFs. For instance, enhanced theta-band oscillations in amygdala have been observed when participants passively view LSF threat faces, while such neural responses are absent when viewing the same faces with broad spatial frequency (BSF) information, despite BSF faces containing LSF components (Maratos, Mogg, Bradley, Rippon, & Senior, 2009). These findings suggest that theta-band oscillations may be modulated by different SFs information during cuteness discrimination tasks. Based on the established relationship between theta-band activity and facial processing, coupled with behavioral findings demonstrating that HSF information facilitates more accurate judgments of facial cuteness levels (Zhou et al., 2023), we hypothesize that significant theta-band activity will be observed, with enhanced responses to HSF faces compared to LSF faces.

Researches in face perception have demonstrated that theta-band oscillations may drive functional connections within a widely distributed system of areas (Dravida et al., 2019; rol Başar, artin Schürmann, & liver Sakowitz, 2001). Importantly, the theta-band connections in posterior area showed enhanced theta-band synchronization when processing emotionally arousing faces. Building upon these findings, we hypothesize that SFs manipulation may similarly modulate theta-band functional connectivity. Specifically, given the established role of HSF information in cuteness perception (Zhou et al., 2023), we predict that HSF faces would elicit stronger posterior theta-band connectivity compared to LSF faces.

Accordingly, this study aims to explore the impact of SFs on cuteness discrimination of infant faces from temporal course. To address this issue, a within-subject experimental design comprising three different SFs conditions was employed. Twenty infant faces with three cuteness levels were selected as faces with BSF. Then, these faces were processed into images with LSF or HSF. Subsequently, two faces with different cuteness levels but same SFs were paired and presented. During EEG recordings, each participant was asked to choose the cuter face from each face pair. Finally, time-domain, time-frequency, and functional connectivity analyses were employed to explore the influence of SFs on different stages of cuteness discrimination.

Method

Participants

Participants were recruited from student volunteers at a university, who were not informed to the experimental purpose. Thirty participants (mean age = 26.39 years, SD = 4.22 years, age range 22-40 years; 8 males and 22 females) were included in the study. Due to a poor signal-to-noise ratio, defined as a rejected rate of artifact epochs exceeding 20%, four participants were excluded, leaving a final sample of twenty-six participants (mean age = 26.58 years, SD = 4.39 years, age range 22-40 years; 6 males and 20 females). The behavioral data of two participants were lost due to operational errors. All participants were right-handed by self-report and had normal or corrected-to-normal vision. None of them had any past or present neurological disorders. Written informed consent was obtained from all participants prior to the start of the study. The testing procedures were reviewed and approved by the local Medical Ethics Committee.

Stimui

We used 50 composite images of infant faces from the Japanese Cute Infant Face Dataset (Nittono, Ohashi, & Komori, 2022) as face stimuli. These images were transformed into a cuter (+50%) or less cute (-50%) version using Psychomorph software. This resulted in three images differing in cuteness for each individual infant, i.e. faces of high cuteness (+50%), of moderate cuteness (0%) and of low cuteness (-50%). Subsequently, the cuteness level of these 150 face images was rated on a 7-point scale, where 1 = Not cute at all and 7 = Extremely cute, using a questionnaire software platform. Fifty-one respondents (mean age = 25.98 years, SD = 7.29 years, age range 18-50 years; 22 males and 29 females) were invited to participate in this task. The cuteness score for each image was determined by averaging the ratings provided by all respondents. Then, the difference between the average scores of high-cuteness and low-cuteness images was calculated for each infant. The top 20 infants with the highest differences were selected, and their images with three cuteness levels were used in the following experiment.

The main experiment employed a within-subject design with three different conditions: BSF, LSF and HSF. A second-order Butterworth filter was applied to the sixty unfiltered infant faces (BSF) separately to filter the LSF ($0.05\sim0.55$ cycles per degree, cpd) and HSF ($5.5\sim13.5$ cpd) images. The stimuli consisted of 180 greyscale images, including 60 unfiltered images (BSF, selected in the pre-experiment) and 120 filtered images (60 with LSF and 60 with HSF), all scaled to 550×550 pixels. The Figure 1 showed the

example faces with different cuteness levels and SFs.

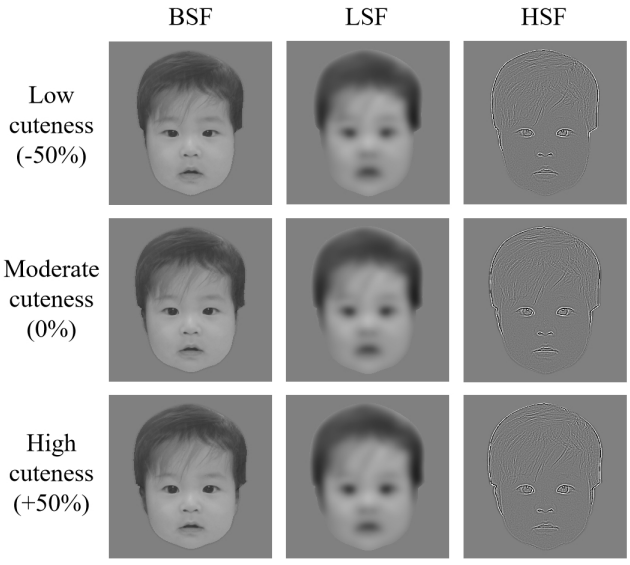

Figure 1: The example faces with different cuteness levels and SFs.

Procedure

Figure 2 illustrates the experimental procedure. Each trial started with a white fixation cross lasting between 1000 and 1400 ms, followed by the presentation of a pair of infant faces for 2000 ms. Pairs of faces were made in a round-robin system (i.e., +50% vs. 0%, 0% vs. -50%, and +50% vs. -50%), with the presented sides (left/right) counter-balanced. Pairs with a large cuteness difference (+50% vs. -50%) were presented twice, while pairs with a smaller cuteness difference (+50% vs. 0%, 0% vs. -50%) were presented once. A pair of faces from the same infant at identical SF was shown, one each on the left and right side of the screen. Images with different SFs were presented in a random order. Participants were instructed to indicate which of two simultaneously presented faces they regarded as cuter. If participants regarded the image presented on the left as cuter, they pressed the "1" key on the numeric keypad of a keyboard with their right hand. Conversely, if they regarded the image presented on the right as cuter, they pressed the "2" key with their right hand.

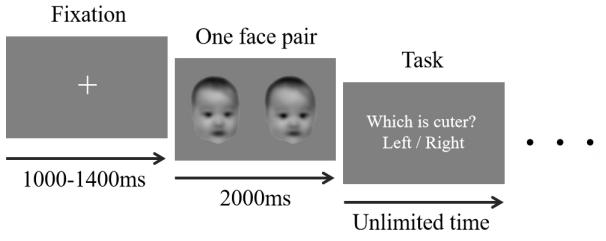

Figure 2: The experimental procedure.

Before the experiment, participants completed 20 practice trials to familiarize themselves with the task. During the main experiment, they were instructed to maintain eye fixation on the center of the screen to avoid unnecessary eye movements throughout the whole of the trial. Participants performed 6 blocks of 80 trials (480 trials in total). After one block, participants could take short breaks. An entire session took around 30-40 min with an additional setup time of 20 min.

We used Psychtoolbox to present the stimuli on a 19-inch DELL P1917S computer monitor with a screen resolution of 1280×1024 and a refresh rate of 60 Hz. The monitor was located at a distance of 50 cm from the participants and a chin rest was used to stabilize the head. Facial stimulus subtended a width of 32.40° of visual angle and a height of 16.40° of visual angle.

EEG Recording and Pre-processing

EEG data were collected in an electrically isolated, light-attenuated room using 34 AgCl electrodes mounted on an electrode cap according to the international 10-10 electrode system. Reference electrodes were placed on both earlobes, and an earth electrode was positioned on the AFz. Eye movements were monitored using a horizontal bipolar electrode (HEOG) placed approximately 1.5 cm from the outer canthi of the left eye and a vertical bipolar electrode (VEOG) placed approximately 1.5 cm below the left eye. The EEG was digitized at a sampling rate of 512 Hz. Electrode impedance was maintained below 10 kΩ.

Offline EEG preprocessing was performed with the EEGLAB v2019.1 toolbox (Delorme & Makeig, 2004) and Letswave 7 (https://letswave.cn/index.html) in MATLAB R2018b (MathWorks, USA). After a 0.1-30 Hz band-pass filtering of the raw EEG data, the data were visually inspected for paroxysmal and muscular artifacts not related to eye blinks, which were then excluded from further analysis. Highly contaminated channels removed during the bad channel rejection were repopulated through spherical interpolation. Thereafter, independent component analysis (ICA) was computed to isolate artifacts in the EEG signal (except for HEOG, VEOG, M1 and M2) using the logistic infomax ICA algorithm in runica function of EEGLAB. Subsequently, cleaned EEG data were segmented ranging from -1000 to 2000 ms relative to the onset of the stimulus. Additionally, we performed a artifact rejection at a strict threshold (±100 μV) and recomputed the reference offline based on the average of all electrodes except for HEOG, VEOG, M1 and M2. After re-referencing, the trials were baseline-corrected using the 200 ms pre-stimulus time window. The number of trials remaining after EEG processing for each condition was approximately of 65.5 trials. A total of 2111 epochs were rejected in all participants, which consisted of artifact epochs and error responses epochs.

Data Analysis

Behavioral Analysis

To examine how response accuracy was influenced by different SFs, accuracy was calculated for each of the three conditions: BSF, LSF, and HSF.

ERPs Analysis

Three clear visual ERP components were analyzed: the P1, the N170, and the P300. The P1, peaking between 95 and 155 ms post-stimulus, and the N170, occurring between 155 and 220 ms after stimulus onset, both exhibited maximal amplitudes over posterior electrodes (P7, P8, P3, P4, O1, O2). Based on this, we computed the mean amplitude for each component separately by averaging the activity across these six electrodes. The P300 was observed within the interval between 250 and 320 ms after stimulus onset. We applied the same analytical procedures to the P300, restricting the analysis to its specific electrode sites (P3, P4, Pz, O1, O2, Oz). Our selection of electrode sites to be included in the ERP analyses was based on prior comparable work (Jessen & Grossmann, 2017; Ohmann et al., 2016) and visual inspection of the topographical distribution of the ERP components with different conditions.

Time-frequency Analysis

Time-frequency analysis was conducted for each participant and condition on a single-trial basis. A short-time Fourier transform was applied with a 300 ms time window, considering the time range from -1000 to 2000 ms (relative to the stimulus onset) and the frequency range from 1 to 30 Hz, with a resolution of 1 Hz. Subsequently, time-frequency representations were averaged across trials for each participant and condition separately. The relative power for each frequency was computed by subtracting the average baseline power (-850 ms to -150 ms from stimulus onset). Finally, the mean power was extracted in specific time and frequency window for further statistical analysis. The electrode clusters of interest included 8 sites: P7, P8, P3, P4, Pz, O1, O2, and Oz. The region of interest (ROI) was defined from 95 to 320 ms after stimulus onset in the 4-8 Hz frequency range, where stronger power was observed.

Functional Connectivity Analysis

The weighted phase lag index (wPLI) was used to measure functional connectivity. This connectivity measure is computed as the weighted phase leads and lags by the magnitude of the imaginary component of the cross-spectrum. The electrode clusters of interest were completely consistent with time-frequency analysis. The connectivity within posterior electrodes was calculated by averaging the matrix cells across all electrode pairs (P7, P8, P3, P4, Pz, O1, O2, Oz). The selection of time and frequency window was in keeping with the time-frequency analysis.

Statistical Analysis

We analyzed participants' behavioral data (accuracy) using a one-way repeated-measures analysis of variance (ANOVA) with SFs (BSF, LSF, HSF) as a within-subject factor. For the ERP data, mean activities measured at the respective electrode sites within each cluster were averaged, and a one-way ANOVA was conducted with SFs as a within-subject factor. Similarly, a one-way ANOVA was performed for time-frequency analysis, with the exception that the mean power in a specific time and frequency range was considered as the dependent variable. The procedure for statistical analysis of functional connectivity was similar to time-frequency analysis.

All analyses were carried out in R 4.3.1. If Mauchly's test of sphericity was violated, the degrees of freedom were adjusted using Greenhouse–Geisser correction. Post hoc analysis were performed with Bonferroni correction. Effect sizes were estimated with partial eta squared (η_p^2) and Cohen's d. The alpha significance value used was 0.05.

Results

Behavioral Results

As shown in Figure 3, the analysis of response accuracy revealed a significant effect of SFs ($F(1.875, 43.119) = 11.751$, $p < .001$, $\eta_p^2 = 0.338$). Specifically, accuracy for BSF was significantly higher than filtered SFs (LSF: $t(23) = -4.722$, $p < .001$, $d = -0.863$; HSF: $t(23) = -3.741$, $p = .003$, $d = -0.851$). In addition, there was no difference between LSF and HSF ($p > .05$).

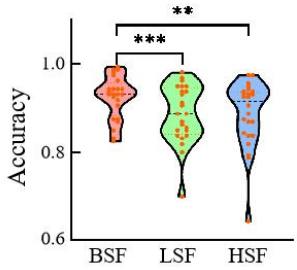

Figure 3: Behavioral performance accuracy.

ERPs Results

Figure 4 illustrates the ERPs results from selected electrodes under three SFs conditions.

P1. Regarding the difference in mean amplitudes among all SFs conditions ($F(1.882, 47.038) = 19.037$, $p < .001$, $\eta_p^2 = 0.432$), BSF and LSF faces elicited larger amplitudes compared to HSF faces (BSF: $t(25) = -5.203$, $p < .001$, $d = -1.047$; LSF: $t(25) = -4.912$, $p < .001$, $d = -1.049$). However, P1 amplitude did not differ between BSF and LSF conditions. ($p > .05$).

N170. Our analysis of mean amplitudes of the N170 revealed a significant main effect of SFs ($F(1.216, 30.402) =$

39.930, $p < .001$, $\eta_p^2 = 0.615$), reflecting that, overall, a larger amplitude in response to HSF than to any of the other two conditions (LSF: t(25) = -5.586, $p < .001$, d = -1.215; BSF: t(25) = -6.966, $p < .001$, d = -1.701). In addition, the amplitude was larger for LSF condition than for BSF condition (t(25) = -5.301, $p < .001$, d = -0.486).

P300. With regard to P300, our analysis yielded a significant main effect of SFs (F(1.776, 44.393) = 11.414, $p < .001$, $\eta_p^2 = 0.313$). The difference in mean amplitudes became significant when faces with BSF (t(25) = -5.087, $p < .001$, d = -0.846) or HSF (t(25) = 3.415, $p < .01$, d = 0.772) were compared to those with LSF. No significant difference was found between BSF and HSF ($p > .05$).

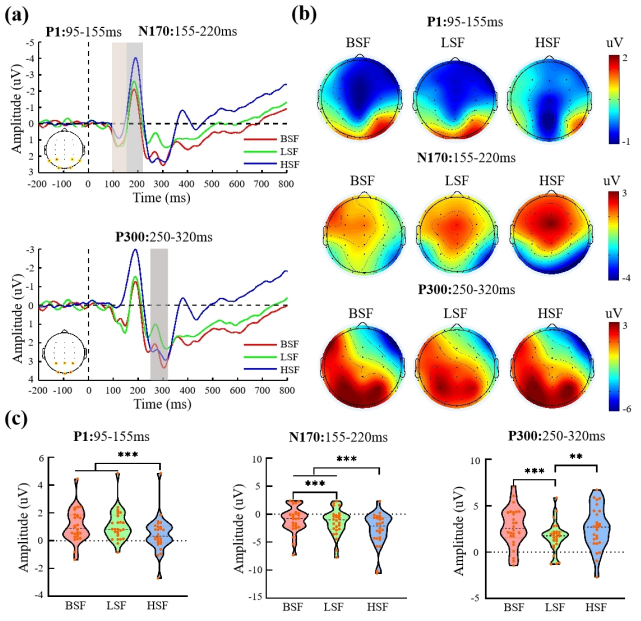

Figure 4: The ERPs results. (a) The grand-averaged ERPs waveforms. The red dots on scalp topography represent analyzed electrodes. The time windows are indicated by shaded areas. (b) Scalp distribution of mean amplitudes at selected time intervals. (c) The three violin plots indicate the difference in mean amplitudes among three SFs conditions. * $p < .05$. ** $p < .01$. *** $p < .001$.

Time-frequency Results

Figure 5 shows the time-frequency results from selected electrodes under three SFs conditions. A stronger power can be observed in a time-frequency window spanning 95-320 ms after stimulus onset in the frequency range 4 to 8 Hz (theta-band). The theta-band activity showed a significant SFs effect in 95-320 ms time window (F(1.331, 33.268) = 22.424, $p < .001$, $\eta_p^2 = 0.473$). The effect reflected greater power for HSF than for LSF (t(25) = 5.108, $p < .001$, d = 1.047) and BSF (t(25) = 4.936, $p < .001$, d = 1.210). Furthermore, the power in LSF condition did not differ from that in BSF condition ($p > .05$).

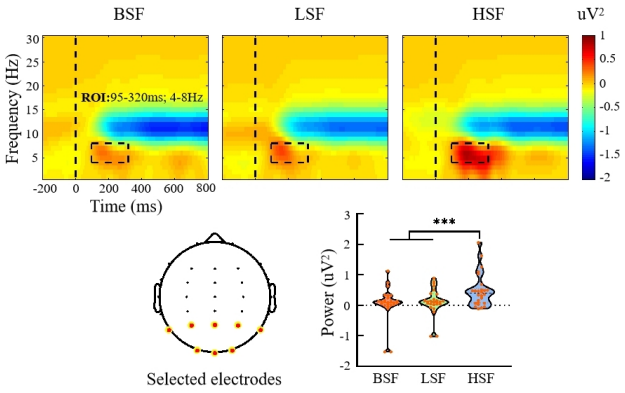

Figure 5: The time-frequency analysis results.

Functional Connectivity Results

Figure 6 illustrates the functional connectivity results under three SFs conditions. Our analysis of functional connectivity in posterior electrodes during 95-320 ms after stimulus onset in 4-8 Hz frequency band range revealed a significant main effect of SFs (F(1.468, 36.707) = 11.405, $p < .001$, $\eta_p^2 = 0.313$). A main SFs effect was explained by a larger wPLI in response to HSF than to LSF (t(25) = 3.708, $p < .01$, d = 0.800) and BSF (t(25) = 3.563, $p < .01$, d = 0.822). Moreover, no significant difference was found between LSF and BSF condition ($p > .05$).

Discussion

The present study investigated how LSF and HSF contribute to the comparison of cuteness between two infant faces by behavioral accuracy measurement, the analysis of time domain, time-frequency and functional connectivity on recorded EEG signals. The behavioral results indicated that participants' cuteness discrimination ability in BSF condition was higher than that in LSF and HSF conditions. Additionally, the ERP analysis revealed that significantly enhanced P1 amplitude responses were observed for LSF faces, while HSF faces elicited greater N170 and P300 amplitude responses. Furthermore, the stronger theta-band oscillations and connectivity in posterior electrodes were observed in HSF condition than that in LSF and BSF. These findings suggest distinct neural mechanisms underlying the processing of SFs information during cuteness discrimination of infant faces.

The behavioral results demonstrated that participants exhibited significantly higher accuracy in cuteness discrimination when viewing BSF faces compared to those containing only LSF or HSF information. This finding is consistent with previous studies on face processing, where the integration of distinct SFs information is critical for constructing a holistic and coherent face perception (Entzmann, Guyader, Kauffmann, Peyrin, & Mermillod, 2023; Freeman & Loschky, 2011; Zhou et al., 2023). Notably, one previous study advanced this understanding by revealing that information in different SFs conditions needs to be integrated in the brain

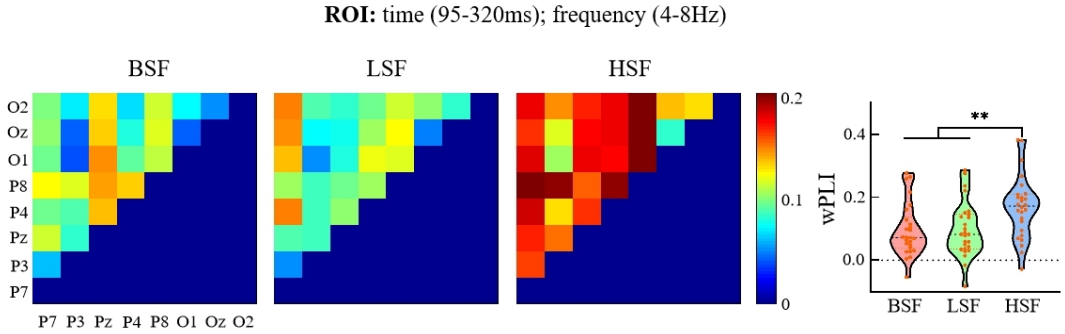

Figure 6: The functional connectivity results.

according to different weights to form the cuteness perception (Zhou et al., 2023). Therefore, the absence of either HSF or LSF information results in a significant reduction in cuteness discrimination accuracy.

The ERP analysis revealed distinct neural processing patterns of LSF and HSF information, characterized by significantly enhanced P1 amplitude observed in response to LSF faces, whereas HSF faces elicited more pronounced N170 and P300 amplitudes. This differential pattern suggests a temporal dissociation of LSF and HSF within the visual system. The enhanced P1 amplitude for LSF faces suggests that early visual system is particularly sensitive to coarse information, which may facilitate the rapid attention capture to infant faces and initial evaluation of cuteness (Bruchmann, Schindler, Dinyarian, & Straube, 2022; Schindler, Wolf, Bruchmann, & Straube, 2021). In contrast, the more pronounced N170 and P300 amplitudes evoked by HSF faces indicate a later, more detailed analysis of facial features. Specifically, the N170 is involved in the encoding of specific facial details, that are critical for discriminating subtle differences in cuteness (Han et al., 2022; H. Wang et al., 2023). The subsequent greater P300 amplitude for HSF faces may be associated with higher-order cognitive processes such as decision-making and evaluation (Proverbio et al., 2023; Shah et al., 2018; Wu et al., 2012). This process may involve a series of cognitive operations such as comparing the facial features of the two presented faces, weighing the significance of each detail in relation to cuteness, and finally making a decision.

Time-frequency and functional connectivity analysis demonstrated that enhanced theta-band oscillations and increased connectivity in posterior area specifically during the processing of HSF faces. This neural signature may reflect the critical role of fine-grained facial features in cuteness discrimination. According to Lorenz's baby schema (1943), infants with a small nose and mouth, large eyes, a round face, and a high forehead are consistently considered cuter than those with a large nose and mouth, small eyes, a narrow face, and a low forehead (Kringelbach, Stark, Alexander, Bornstein, & Stein, 2016). In general, these detailed features essential for cuteness discrimination are more prevalent in HSF faces than that in LSF faces (Øvervoll, Schettino, Suzuki, Okubo, & Laeng, 2020; Vuilleumier, Armony, Driver, & Dolan, 2003). Therefore, allocating more attention resources in HSF faces may be more conducive to achieve cuteness discrimination. This enhanced attentional engagement is manifested through stronger theta-band oscillations, which facilitate the integration of visual and emotional information across distributed neural networks (Dravida et al., 2019; rol Başar et al., 2001). Consequently, the observed pattern of enhanced theta-band activity and connectivity in the HSF condition may represent a neural mechanism underlying successful cuteness discrimination, where the visual system prioritizes the processing of detailed facial features that are most informative for cuteness judgment.

Acknowledgments

This work was supported by the National Natural Science Foundation of China (62376184, 62303445, and 62206196), Central Guided Local Science and Technology Development Project (YDZJSX20231A017), and Shenzhen Science and Technology Program (JCYJ20230807140719040).

References

Almanza-Sepúlveda, M. L., Dudin, A., Wonch, K. E., Steiner, M., Feinberg, D. R., Fleming, A. S., & Hall, G. B. (2018). Exploring the morphological and emotional correlates of infant cuteness. *Infant Behavior and Development*, *53*, 90–100.

Borgi, M., Cogliati-Dezza, I., Brelsford, V., Meints, K., & Cirulli, F. (2014). Baby schema in human and animal faces induces cuteness perception and gaze allocation in children. *Frontiers in psychology*, *5*, 411.

Bossi, F., Premoli, I., Pizzamiglio, S., Balaban, S., Ricciardelli, P., & Rivolta, D. (2020). Theta-and gamma-band activity discriminates face, body and object perception. *Frontiers in Human Neuroscience*, *14*, 74.

Bruchmann, M., Schindler, S., Dinyarian, M., & Straube, T. (2022). The role of phase and orientation for erp modulations of spectrum-manipulated fearful and neutral faces. *Psychophysiology*, *59*(3), e13974.

Delorme, A., & Makeig, S. (2004). Eeglab: an open source toolbox for analysis of single-trial eeg dynamics including independent component analysis. *Journal of neuroscience methods*, *134*(1), 9–21.

Di Lorenzo, R., Munsters, N. M., Ward, E. K., de Jonge, M., Kemner, C., & van den Boomen, C. (2021). Is it fear? similar brain responses to fearful and neutral faces in infants with a heightened likelihood for autism spectrum disorder. *Journal of autism and developmental disorders*, *51*, 961–972.

Dravida, S., Ono, Y., Noah, J. A., Zhang, X., & Hirsch, J. (2019). Co-localization of theta-band activity and hemodynamic responses during face perception: simultaneous electroencephalography and functional near-infrared spectroscopy recordings. *Neurophotonics*, *6*(4), 045002–045002.

Entzmann, L., Guyader, N., Kauffmann, L., Peyrin, C., & Mermillod, M. (2023). Detection of emotional faces: The role of spatial frequencies and local features. *Vision Research*, *211*, 108281.

Freeman, T. E., & Loschky, L. C. (2011). Low and high spatial frequencies are most useful for drawing. *Psychology of Aesthetics, Creativity, and the Arts*, *5*(3), 269.

Han, S., Hu, J., Gao, J., Fan, J., Xu, X., Xu, P., & Luo, Y. (2022). Comparisons make faces more attractive: An erp study. *Brain and Behavior*, *12*(6), e2561.

Jennings, B. J., Yu, Y., & Kingdom, F. A. (2017). The role of spatial frequency in emotional face classification. *Attention, Perception, & Psychophysics*, *79*, 1573–1577.

Jessen, S., & Grossmann, T. (2017). Exploring the role of spatial frequency information during neural emotion processing in human infants. *Frontiers in human neuroscience*, *11*, 486.

Jia, H. M., Park, C. W., & Pol, G. (2015). Cuteness, nurturance, and implications for visual product design. In *The psychology of design* (pp. 168–179). Routledge.

Kringelbach, M. L., Lehtonen, A., Squire, S., Harvey, A. G., Craske, M. G., Holliday, I. E., ... others (2008). A specific and rapid neural signature for parental instinct. *PloS one*, *3*(2), e1664.

Kringelbach, M. L., Stark, E. A., Alexander, C., Bornstein, M. H., & Stein, A. (2016). On cuteness: Unlocking the parental brain and beyond. *Trends in cognitive sciences*, *20*(7), 545–558.

Lin, H., & Liang, J. (2024). Comparison with others influences encoding and recognition of their faces: behavioural and erp evidence. *NeuroImage*, *288*, 120538.

Lin, H., & Liang, J. (2025). Competition modulates the effects of social comparison on erp responses during face processing. *Social Cognitive and Affective Neuroscience*, *20*(1), nsaf005.

Lin, T., Zhang, X., Fields, E. C., Sekuler, R., & Gutchess, A. (2022). Spatial frequency impacts perceptual and attentional erp components across cultures. *Brain and cognition*, *157*, 105834.

Lorenz, K. (1943). Die angeborenen formen möglicher erfahrung. *Zeitschrift für Tierpsychologie*, *5*(2), 235–409.

Maratos, F. A., Mogg, K., Bradley, B. P., Rippon, G., & Senior, C. (2009). Coarse threat images reveal theta oscillations in the amygdala: A magnetoencephalography study. *Cognitive, Affective, & Behavioral Neuroscience*, *9*(2), 133–143.

Maurer, D., Le Grand, R., & Mondloch, C. J. (2002). The many faces of configural processing. *Trends in cognitive sciences*, *6*(6), 255–260.

Miesler, L., Leder, H., & Herrmann, A. (2011). Isn't it cute: An evolutionary perspective of baby-schema effects in visual product designs. *International Journal of Design*, *5*(3).

Nittono, H., Ohashi, A., & Komori, M. (2022). Creation and validation of the japanese cute infant face (jcif) dataset. *Frontiers in Psychology*, *13*, 819428.

Ohmann, K., Stahl, J., Mussweiler, T., & Kedia, G. (2016). Immediate relativity: Eeg reveals early engagement of comparison in social information processing. *Journal of Experimental Psychology: General*, *145*(11), 1512.

Øvervoll, M., Schettino, I., Suzuki, H., Okubo, M., & Laeng, B. (2020). Filtered beauty in oslo and tokyo: A spatial frequency analysis of facial attractiveness. *Plos one*, *15*(1), e0227513.

Parsons, C. E., Young, K. S., Mohseni, H., Woolrich, M. W., Thomsen, K. R., Joensson, M., ... Kringelbach, M. L. (2013). Minor structural abnormalities in the infant face disrupt neural processing: a unique window into early caregiving responses. *Social neuroscience*, *8*(4), 268–274.

Pfabigan, D. M., Wucherer, A. M., Wang, X., Pan, X., Lamm, C., & Han, S. (2018). Cultural influences on the processing of social comparison feedback signals—an erp study. *Social Cognitive and Affective Neuroscience*, *13*(12), 1317–1326.

Proverbio, A. M., Cerri, A., & Gallotta, C. (2023). Facemasks selectively impair the recognition of facial expressions that stimulate empathy: an erp study. *Psychophysiology*, *60*(8), e14280.

Proverbio, A. M., & Zani, A. (2021). Hemispheric asymmetry in visual processing: An erp study on spatial frequency gratings. *Symmetry*, *13*(2), 180.

rol Başar, E., artin Schürmann, M., & liver Sakowitz, O. (2001). The selectively distributed theta system: functions. *International Journal of Psychophysiology*, *39*(2-3), 197–212.

Schindler, S., Wolf, M.-I., Bruchmann, M., & Straube, T. (2021). Fearful face scrambles increase early visual sensory processing in the absence of face information. *European Journal of Neuroscience*, *53*(8), 2703–2712.

Senese, V. P., De Falco, S., Bornstein, M. H., Caria, A., Buffolino, S., & Venuti, P. (2013). Human infant faces provoke implicit positive affective responses in parents and non-parents alike. *PloS one*, *8*(11), e80379.

Shah, D., Knott, V., Baddeley, A., Bowers, H., Wright, N.,

Labelle, A., … Collin, C. (2018). Impairments of emotional face processing in schizophrenia patients: Evidence from p100, n170 and p300 erp components in a sample of auditory hallucinators. *International Journal of Psychophysiology*, *134*, 120–134.

Thompson-Booth, C., Viding, E., Mayes, L. C., Rutherford, H. J., Hodsoll, S., & McCrory, E. J. (2014). Here's looking at you, kid: Attention to infant emotional faces in mothers and non-mothers. *Developmental science*, *17*(1), 35–46.

Torrence, R. D., Troup, L. J., Rojas, D. C., & Carlson, J. M. (2021). Enhanced contralateral theta oscillations and n170 amplitudes in occipitotemporal scalp regions underlie attentional bias to fearful faces. *International Journal of Psychophysiology*, *165*, 84–91.

Vuilleumier, P., Armony, J. L., Driver, J., & Dolan, R. J. (2003). Distinct spatial frequency sensitivities for processing faces and emotional expressions. *Nature neuroscience*, *6*(6), 624–631.

Wang, H., Lian, Y., Wang, A., Chen, E., & Liu, C. (2023). Face motion form at learning influences the time course of face spatial frequency processing during test. *Biological Psychology*, *183*, 108691.

Wang, T., Mukhopadhyay, A., & Patrick, V. M. (2017). Getting consumers to recycle now! when and why cuteness appeals influence prosocial and sustainable behavior. *Journal of Public Policy & Marketing*, *36*(2), 269–283.

Williams, N. R., Willenbockel, V., & Gauthier, I. (2009). Sensitivity to spatial frequency and orientation content is not specific to face perception. *Vision Research*, *49*(19), 2353–2362.

Wu, Y., Zhang, D., Elieson, B., & Zhou, X. (2012). Brain potentials in outcome evaluation: when social comparison takes effect. *International Journal of Psychophysiology*, *85*(2), 145–152.

Yang, Y., Qiu, Y., & Schouten, A. C. (2015). Dynamic functional brain connectivity for face perception. *Frontiers in Human Neuroscience*, *9*, 662.

Zhang, Z., & Zhou, J. (2020). Cognitive and neurological mechanisms of cuteness perception: A new perspective on moral education. *Mind, Brain, and Education*, *14*(3), 209–219.

Zhou, M., Li, H., Li, Q., Uehara, T., Yao, L., Yang, J., … Wu, J. (2023). Spatial frequencies affect cuteness perception of infant faces. *Emotion*, *23*(2), 512.